A Saturable Pulse Transformer Based on Nanocrystalline Magnetic Cores for an Adjustable Nanosecond High-Voltage Generator

Mawuena Degnon, Anton Gusev, Antoine Silvestre de Ferron, Laurent Pecastaing, Aleksandr Baranov, Christophe Mielot, Sébastien Boisne, Michael Barnes, Viliam Senaj, Thomas Kramer, et al.

A Saturable Pulse Transformer Based on Nanocrystalline Magnetic Cores for an Adjustable Nanosecond High-Voltage Generator

Mawuena R. Degnon, *Student Member, IEEE*, Anton Gusev, *Member, IEEE*, Antoine Silvestre de Ferron, Laurent Pecastaing, *Senior Member, IEEE*, Aleksandr Baranov, Christophe Mielot, Sébastien Boisne, Michael Barnes, Viliam Senaj, Thomas Kramer, and Bucur M. Novac, *Senior Member, IEEE*

***Abstract*—This paper is devoted to saturable pulse transformers (SPTs), combining the functions of a pulse transformer and a magnetic switch. Two nanocrystalline magnetic cores are investigated in the SPT of an inductive energy storage (IES) pulsed power system based on a semiconductor opening switch (SOS). The first magnetic core has a square hysteresis loop (Br/Bsat > 90%), while the second core has a flat hysteresis loop (Br/Bsat ~4%). A test bench with an initially stored energy of 10 J is developed. The circuit design is discussed, and the magnetic materials are compared. Based on the features of the hysteresis loops, two nanosecond high-voltage SOS generators are tested, with the output voltage adjusted by tuning the input voltage and controlling the bias magnetic field. The influence of the optimal core saturation on the operation of the SOS diode is studied. An adjustable output voltage impulse of more than 200 kV amplitude with a 16 ns rise time is demonstrated on a 1 kΩ resistive load.**

***Index Terms* — Nanocrystalline magnetic core, pulsed power systems, saturable pulse transformer, semiconductor opening switch.**

I. INTRODUCTION

THE advent of semiconductor opening switches (SOSs) discovered in the 1990s [1] has opened the gate for solid-state pulsed power based on the inductive energy storage (IES) technique. Recently, high-voltage nanosecond generators based on SOS diodes, so-called SOS generators, are becoming increasingly attractive for repetitive pulsed power applications. These systems have many advantages, such as high pulse repetition frequency, high reliability, and long lifetime, and are mainly used both in basic research and in major industrial applications such as high-power microwaves, pulsed HV gas, vacuum and underwater plasma electrical discharges, particle acceleration, X-ray devices, and many others [2]–[6].

From a structural viewpoint, the SOS generators usually involve magnetic elements, used in voltage-boosting pulse transformers and magnetic pulse compressors (MPCs) [2], [7]–[10]. The robustness, stability, high-frequency operation, and long lifetime of magnetic elements [11]–[21], make these items suitable for use in solid-state generators. A noteworthy illustration is their utilization in the injection and extraction systems utilized in state-of-the-art particle accelerator facilities [21], [22]. In addition, the use of multiple MPC stages enables reducing the stress on the primary solid-state switch while keeping a high voltage output, although the efficiency might be compromised [12]–[14], [17]. It is well known that the material of the magnetic element strongly affects the efficiency of the generator, especially at the fast magnetization that is particularly required for SOS generators.

Furthermore, adjustment of the output voltage level is often required in pulsed power applications including x-ray, e-beam, excimer lasers, generation of ozone, and others [12], [23]. In [18] and [23], the output voltage was adjusted by varying the input voltage, while using either a Fe-based amorphous or a permalloy magnetic core pulse transformer, respectively. However, the absence of a pre-magnetizing circuit introduces limits on the voltage regulation range and energy efficiency. The work [19] proposed a method to regulate the peak voltage, the saturation time, and the pulse compression ratio, using different connection points of the magnetic switch winding to adjust the number of turns. However, this approach appears to be complex when a large number of connection points is required. A novel topology was suggested by [8] in which an additional primary circuit connected to the primary winding is

This work was supported in part by the French "Investissements d'Avenir" Program within the Framework of the Energy and Environment Solutions-Université de Pau et des Pays de l'Adour (E2S UPPA) Project [Solid-State Pulsed Power (S2P2) and Pulsed Power Applications (PULPA) Chairs] managed by the Agence Nationale de la Recherche (ANR) under Grant ANR-16-IDEX-0002 and in part by ITOPP ALCEN.

M. R. Degnon is with the SIAME Laboratory, Université de Pau et des Pays de l'Adour, E2S UPPA, 64000, Pau, France, and also with ITOPP ALCEN, 46500 Thégra, France (e-mail: rdegnon@itopp-alcen.com).

A. Gusev, A. Silvestre de Ferron, and L. Pecastaing are with the SIAME Laboratory, Université de Pau et des Pays de l'Adour, E2S UPPA, 64000, Pau, France (e-mail: anton.gusev@univ-pau.fr).

A. Baranov, C. Mielot, S. Boisne are with ITOPP ALCEN, 46500, Thégra, France (e-mail: abaranov@itopp-alcen.com).

M. Barnes, V. Senaj, T. Kramer are with CERN, CH-1211, Geneve 23, Switzerland (e-mail: mike.barnes@cern.ch).

B. M. Novac is with the Wolfson School of Mechanical, Electrical and Manufacturing Engineering, Loughborough University, Loughborough, Leicestershire LE11 3TU, U. K, and also with the SIAME Laboratory, Université de Pau et des Pays de l'Adour, E2S UPPA, 64000, Pau, France (e-mail: b.m.novac@lboro.ac.uk).

used to reset the core. In this configuration though, the input voltage remains unchanged, which may lower the efficiency.

The present work studies a saturable pulse transformer (SPT) with a controlled time to saturation, as part of a high-efficiency adjustable SOS generator. A circuit containing a single magnetic element, an SPT, is used to ensure high efficiency.

In a single magnetic element SOS generator, an SPT combines two functions: (i) a step-up transformer with an energy transfer time of about 500 ns, and (ii) a magnetic switch with a current compression ratio of about 2.5. Nanocrystalline soft magnetic materials, presenting a high saturation induction, low magnetic losses, high permeability, and high resistivity, meet all the requirements for a highly efficient SPT [13], [24], [25]. Nanocrystalline MPCs were used in our recently published study [26], where off-the-shelf diodes were examined as high-voltage solid-state opening switches. The present paper is centered on the SPT-based system in general, while also using an SOS diode. It is therefore focused on two types of nanocrystalline magnetic cores with different shapes of the hysteresis loop (i.e., B-H curve). The first type has a flat loop (i.e., a low remanent induction), which is traditionally used in transformers. The second type has a square hysteresis loop (i.e., a high remanent induction), which is a well-known characteristic of magnetic materials used in pulsed power magnetic switches. These magnetic materials are investigated when used in a single-core transformer topology, to compare their efficiency and suitability for the SPT of the SOS generator. To this end, a test bench with an initially stored energy of 10 J, is developed.

The paper is structured as follows. In Section II, the design of the pulse transformer, the operating principle of the SOS generator, and the characteristics of the nanocrystalline magnetic cores are described. In Section III, the results obtained using the two different magnetic materials are compared and discussed. In the same section, the high-voltage SOS generators are presented. The paper ends with the Conclusion and the suggested way ahead.

II. Circuit Principle and System Design

A. General Layout and Operating Principle of the Circuit

The general layout of the test bench is presented in Fig. 1. The arrangement consists of a triggered spark gap switch SG and a film capacitor C1, connected to the primary winding of the SPT. The secondary winding of the transformer is connected to the low inductive ceramic capacitor C2, followed by the SOS diode and the resistive load R in parallel. The current viewing resistors R_{Sh1} and R_{Sh2}, made in-house from carbon composition resistors, are used for the SOS current and load voltage measurements. The measurement of V_{C1} and V_{C2} is performed using North Star high-voltage probes type PVM-12 and PVM-100, respectively. A pre-magnetizing circuit (magnetic bias circuit) is used to reset the core before each pulse. This circuit comprises a direct current (DC) source (IPS 303A, 0-3 A, 0-30 V) and an in-house made choke, which protects this current source from the main high-voltage pulse. The specifications of the circuit components are described in Table I.

The operating principle of the experimental setup (Fig. 1) is as follows. C1 is charged by an external power supply (for simplicity this is not shown). When SG closes, the energy stored in C1 is transferred to the capacitor C2 through the transformer SPT. The current of amplitude I^+ and duration t^+, termed "forward pumping current", flows through the SOS diode in a forward direction, charging C2. Subsequently, when the voltage across C2 reaches its maximum value, the SPT is designed to saturate. As a result, the secondary winding is decoupled from the primary winding. In addition, the inductance of the secondary winding of the saturated core significantly decreases due to the low permeability of the core in its saturated state. Hence, the discharge current of C2 of higher amplitude I^-, termed "reverse pumping current", flows through the SOS for the duration t^-. In order to reach the reversed current density of several to tens of kA/cm² that is required for the SOS-mode current cut-off [2], a high value of I^- is necessary to be generated. Finally, the high-value reverse current is interrupted by the SOS within the current cut-off time t_0, then the energy is transferred to the load R, generating a nanosecond rise time high-voltage pulse.

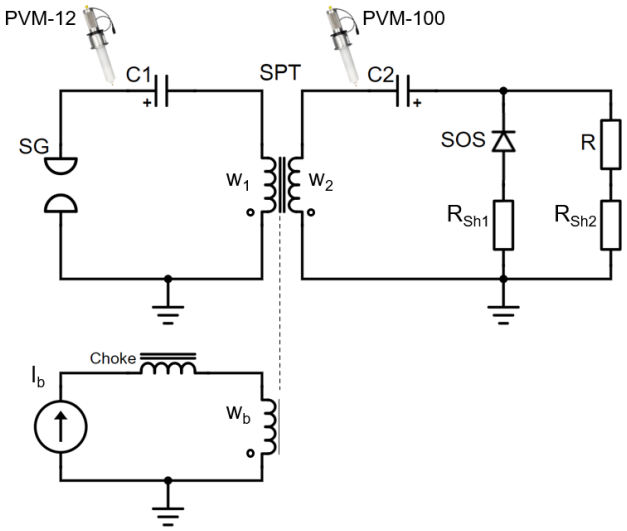

Fig. 1. Circuit diagram of the experimental arrangement.

Table I
Specifications of Circuit Components

	C1	C2	SOS	R	R_{Sh1}	R_{Sh2}
Value	200 nF	2 nF	180 kV/4 kA	0.05–1 kΩ	0.15 Ω	0.5 Ω
Type	STP-02QI	UHV-9A	SOS-180-4	TVO-20	RCC050	

The typical waveforms of the SOS current, the charging voltages V_{C1} of C1 and V_{C2} of C2, and the load voltage V_R are presented in Fig. 2. A non-zero resistance of the SOS in the conductive state causes negative and positive pre-pulses on the load voltage (V_R). This can be suppressed by two oppositely connected diodes in series with the load as described in [27]. However, this topic is beyond the scope of the present work.

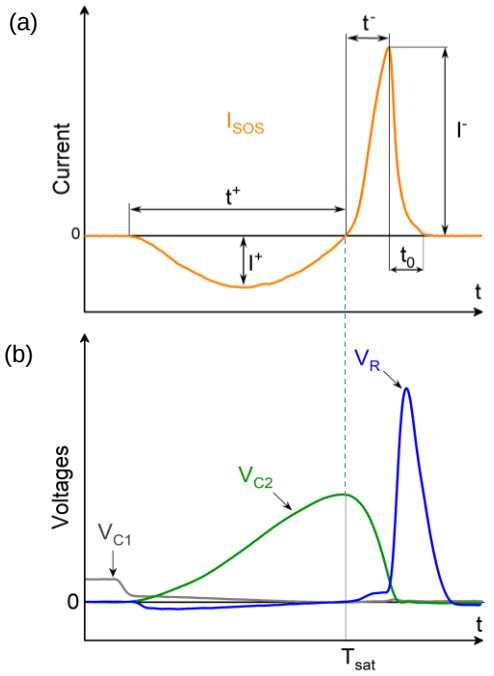

Fig. 2. Typical waveforms of (a) the current flowing through the SOS diode, and (b) the voltages V_{C1}, V_{C2} (reversed for clarity), and V_R.

B. Design of the 100 kV Saturable Pulse Transformer

The 10 kV capacitor C1 set the input energy to 10 J maximum. A toroidal shape of the core is adopted, and the transformation ratio *n* is fixed to 10. To improve energy transfer efficiency, the primary and secondary capacitors are matched as follows:

$$C1 = n^2 \times C2 \tag{1}$$

According to the requirement for an SOS diode pumping as stated in [2] and based on preliminary studies, the forward and reverse pumping durations of the diode were defined respectively as $t^+ = 500$ ns and $t^- = 100$ ns. Therefore, the equivalent capacitance C_{eq} and self-inductance L_{eq} of the transformer, when referring to the primary side, can be estimated as:

$$C_{eq} = \frac{C_1 \times n^2 C_2}{C_1 + n^2 C_2} = \frac{C_1}{2} \tag{2}$$

$$L_{eq} = \frac{(t^+)^2}{\pi^2 \times C_{eq}} \tag{3}$$

where t^+ is the forward pumping time of the SOS. For an ideal energy transfer, t^+ must correspond to the time required for the peak voltage of C2 to be reached and to the saturation time T_{sat} of the transformer (see Fig. 2). In this condition, the size of the core is determined using the simplified form of the Faraday law termed the volt-second product:

$$2\Delta B \times S_c \times w_2 = V_{max} \times T_{sat} \tag{4}$$

where ΔB is the magnetic induction swing, S_c is the effective cross-section area of the material without the interlaminar insulating layers, w_2 is the number of turns of the secondary winding and V_{max} is the peak voltage of C2. S_c is determined by multiplying the geometrical cross-section of the core S_g (see Fig. 3, (1)) by the packing factor k = 0.73, as indicated by the manufacturer. The packing factor represents the ratio of the effective to the geometrical cross-section area of the core, and due to the interlaminar insulation of the wound cores it is always less than 1.

The magnetic induction swing ΔB, representing the change in the magnetic induction, is one of the most crucial parameters to consider when choosing the core material. Indeed, for the same core size, a material with a higher induction swing will lead to a higher energy transfer. In other words, a high saturation flux density implies a low magnetic core volume for the same voltage amplitude across the secondary winding.

As the transformer is operating in air, proper attention should be paid to the electrical insulation. Hence, to prevent an electrical breakdown between the winding and the core, plastic insulating supports are required (see Fig. 3, (2)). The plastic supports were 3D printed using polylactic acid (PLA) filaments. These supports, designed by considering the air dielectric strength as 30 kV/cm, ensure a minimum distance between the winding and the core of 12 mm in all directions. To extend the current path and prevent any surface breakdown, ripples are applied at the two ends of the support sleeves (see Fig. 3, (3)). The transformer windings comprise a single-turn primary (w_1=1) and a 10-turn secondary (w_2=10) windings. The primary winding is made up of a metallic cylinder with a diameter of 100 mm, which is placed in the center of the transformer. The top part of the cylinder is connected to the primary capacitor C1 through a metallic plate. The base of the cylinder is directly connected to the grounded plate underneath the transformer. The secondary winding consists of two parallel sections covering the entire surface of the core. To regulate the induction swing, an additional 5-turn winding is applied, as a part of the pre-magnetizing circuit.

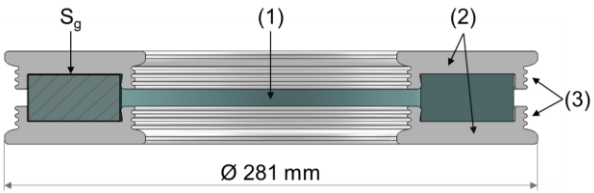

Fig. 3. Sectional view of the SPT showing the cross-section S_g, (1) the core, (2) the PLA supports and (3) the rippled sleeves.

The link between the pre-magnetizing current and the induction is expressed, respectively by (5) and (6):

$$H = \frac{I_b \times w_b}{l_m} \tag{5}$$

$$B = \mu H \tag{6}$$

where H is the bias magnetic field, I_b is the pre-magnetizing

current, w_b is the number of turns of the pre-magnetizing winding, l_m is the mean magnetic path length of the core, B is the induction flux and μ is the magnetic permeability.

C. Overview of the Tested Cores

Two nanocrystalline Fe-based soft magnetic materials were investigated as SPTs. The nanocrystalline cores provide high saturation flux density, high relative permeability, low core loss and excellent temperature characteristics for a wide frequency range [28]. The characteristics of the cores, including the saturation induction B_{sat}, the remanent induction B_r, the coercive force H_c, the magnetic material cross-section S_c and the core size are all provided in TABLE II, and their corresponding B-H loops are presented in Fig. 4.

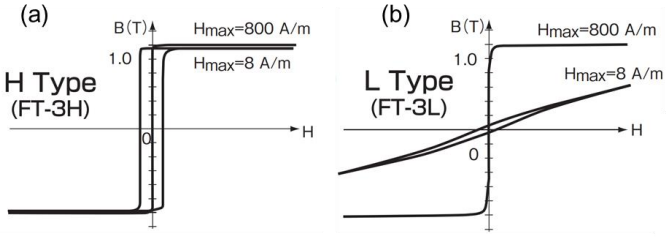

Fig. 4. B-H loops of (a) Finemet FT-3H, and (b) Finemet FT-3L reproduced from [27].

TABLE II
PARAMETERS OF THE PULSE TRANSFORMER CORES

	B_{sat} (T)	B_r/B_{sat}	H_c (A/m)	S_c (cm^2)	Size (mm^3)
Finemet FT-3H	1.23	> 90%	0.6	8.29	256 x 165 x 25
Finemet FT-3L	1.23	4%	0.6	8.29	256 x 165 x 25

III. TEST AND RESULTS

A. Investigation of the Nanocrystalline Magnetic Cores

As described in the previous sections, the parameters of the magnetic core, and particularly the effective induction swing, are critical to minimize the size of the core. However, the static characteristics provided in the manufacturer's datasheet may differ from dynamic characteristics, especially under fast pulse magnetization [13], [29]. Hence, in these experiments, the effective induction swings of the two cores are determined and compared.

To this end, at a fixed input voltage, the bias magnetic field H_0 is continuously applied using the pre-magnetizing circuit, to set the initial induction to B_0. Thus, the total induction swing ΔB can be defined by:

$$\Delta B = B_{sat} - B_0 \leq 2B_{sat} \qquad (7)$$

where the induction swing is obtained using the volt-second product defined in (4). The peak voltage V_{max} of C2 is measured and the saturation time T_{sat} is graphically determined using the SOS current and the V_{C2} waveforms (see Fig. 2).

In these experiments, the input voltage is fixed at 6 kV and the magnetic field H_0 is varied from 0 to 23 A/m, to regulate the induction swing. H_0 is applied in the opposite direction compared to the main pulse, to increase the effective induction swing. The results obtained are plotted in Fig. 5. The error bar corresponds to the inaccuracy in the measurement of the saturation time T_{sat}.

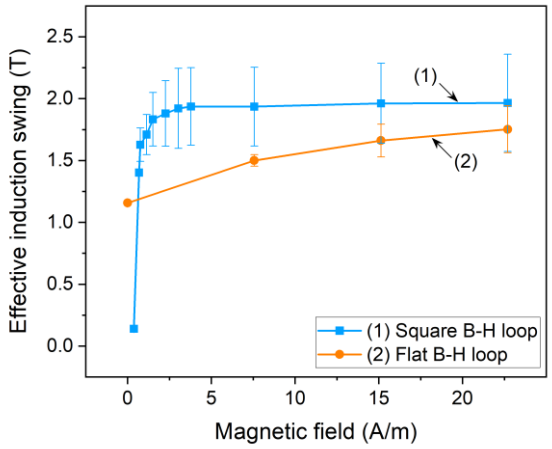

Fig. 5. Effective induction swing of the SPT cores as a function of the bias magnetizing field H_0 for (1) Finemet FT-3H and (2) Finemet FT-3L.

The induction swings obtained when operating the materials under fast pulse magnetization are in good agreement with the datasheet specifications. For the square B-H loop core (i.e., Finemet FT-3H), a maximum induction swing of 2 ± 0.2 T is achieved by applying a low magnetic field of absolute value H_0 about 5 A/m. The further increase in the bias magnetic field does not lead to the increase of the ΔB, which confirms the operation at the maximum induction swing. Hence, the maximum flux density, inducing the highest voltage across the secondary of the transformer (V_{C2}), can be achieved by applying a relatively low bias magnetic field using the square B-H loop core. However, the steep slope of the induction in the area between 0 and 2 A/m (Fig. 5, (1)) seriously reduces the possibility of tuning the ΔB.

On contrary, at the maximum bias magnetic field of 23 A/m, the maximum induction swing obtained while using the flat B-H loop core (i.e., Finemet FT-3L) is 1.75 ± 0.2 T. Even though the remanent induction of the Finemet FT-3L is low (~0.05 T), the continuously applied H_0 makes it possible to achieve a substantial induction swing, close to 2Bsat. Due to the limit of the pre-magnetizing circuit – limited current source and number of turns – the induction swing could not be further increased for this arrangement. However, the smooth slope of the induction curve (Fig. 5, (2)) provides the excellent advantage of regulating the induction swing.

B. Adjustable Nanosecond High-Voltage Generator Based on SOS-180-4 and Finemet FT-3L

The advantage of the flat B-H loop core is harnessed in the development of an adjustable high-voltage SOS generator. The adjustment of the output voltage is performed by changing the input voltage (i.e., the C1 charging voltage V_{C1}). However, to maintain a high efficiency, an optimal pre-magnetizing H_0 should be applied to achieve an optimum saturation. The

optimum saturation corresponds to the situation where the core is saturated at the precise moment when the charging voltage of the secondary capacitor V_{C2} reaches its peak amplitude, and the SOS current is zero (Fig. 2). If saturation occurs too early, it prevents the transmission of all the energy stored in the primary capacitor C1. If saturation occurs too late, a part of the energy transmitted to the secondary capacitor C2 is transferred back to the primary circuit. Therefore, a transformer designed to saturate at the optimum moment ensures an efficient and complete energy transfer from C1 to C2.

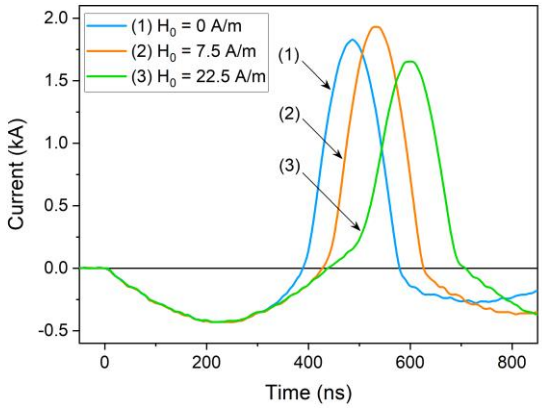

Fig. 6. Waveforms of the current through C2 at different saturation states of the SPT, depending on the bias magnetic fields H_0: (1) early saturation, (2) optimum saturation, and (3) late saturation.

A preliminary study was carried out to determine the optimal pre-magnetizing H_0 for each V_{C1}. In this preliminary study, the diode is short-circuited and the secondary of the transformer consists of the secondary winding in series with the capacitor C2. The input voltage V_{C1} is varied from 3 to 10 kV. For each input voltage, the magnetic field is tuned to obtain the optimum saturation. Fig. 6 presents the three different states of early, optimum, and late saturation. It is shown that the reverse current is at its maximum when the saturation time is optimal. Consequently, the reverse pumping current density required for the SOS effect is improved when operating at the optimum saturation. For the input voltage of 7 kV, the optimum magnetic field applied is 7.5 A/m for which a maximum reversed current amplitude of 1.9 kA is obtained (see Fig. 6, (2)).

TABLE III
PARAMETERS OF THE ADJUSTABLE HIGH-VOLTAGE GENERATOR

V_{C1} (kV)	3	4	5	6	7	8	9	10
H_0 (A/m)	-	-	-	7.5	7.5	15	15	22.5
$\|V_{C2}$ (kV)$\|$	24	32	40	48	56	63	72	80
V_R (kV)	10	22	30	38	44	50	55	60
$t_{R(0.1\text{-}0.9)}$ (ns)	39	25	22	21	19	18	16	16
FWHM (ns)	85	63	60	57	55	55	54	53
η_{PT} (%)	65	67	66	70	68	69	70	68

Based on this preliminary study, an adjustable SOS generator, having an electrical circuit shown in Fig. 1, was designed and manufactured. The generator components are the same as described in TABLE I. A single core of Finemet FT-3L is used for the saturable pulse transformer, whose design parameters are as described in Section II.B. The resistive load is set to 50 Ω as an example. For insulation considerations, both the diode and the load are immersed in oil.

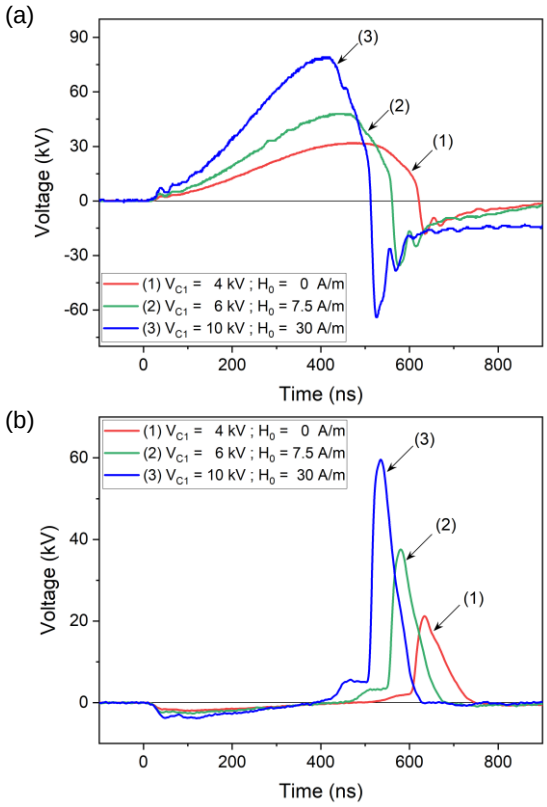

Fig. 7. Typical waveforms of (a) secondary capacitor voltage V_{C2} (reversed for clarity) and (b) load voltage V_R, when the primary capacitor is charged to 4 kV, 6 kV, and 10 kV.

The typical waveforms of V_{C2} and V_R are shown in Fig. 7 for different values of V_{C1} and H_0. Fig. 8 presents the voltage amplitudes of the V_{C2} and V_R as a function of V_{C1}. By varying the input voltage from 3 kV to 10 kV, V_{C2} is changed from 24 kV to 80 kV and the output load voltage is adjusted almost linearly from 10 kV to 60 kV. The proper bias magnetic field is also applied, to ensure the optimum saturation is reached at each operation point. Although the rise time and duration of the load voltage are shortened with the voltage increase, these parameters are hardly tunable in this circuit. Therefore, the adjustment described in this paper is only related to the amplitude of the output voltage.

The main characteristics of the adjustable high-voltage generator working on 50 Ω load are summarized in TABLE III, including the load voltage pulse parameters: peak amplitude V_R, rise time $t_{R(0.1\text{-}0.9)}$, and full width at half maximum (FWHM). The transformer efficiency η_{PT} is evaluated as the ratio of primary and secondary stored energy (8):

$$\eta_{PT} = \frac{E_{C2}}{E_{C1}} \tag{8}$$

It is worth noting that this efficiency includes spark gap losses. Therefore, the ultimate efficiency of the transformer itself is

likely to be higher than the calculated η_{PT}. Thanks to the regulation of the induction swing, the transformer efficiency remains almost constant for all the output voltages (see TABLE III); its value of up to 70% was calculated using (8).

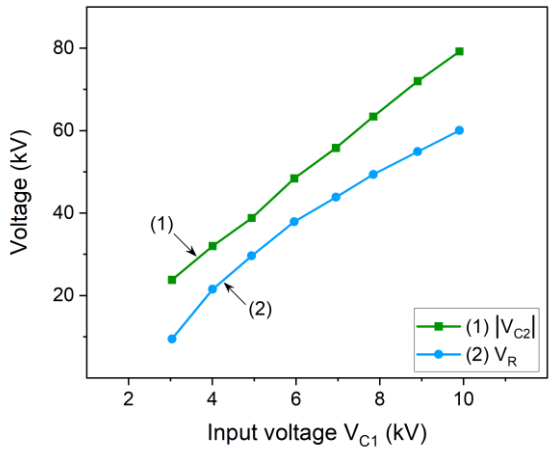

Fig. 8. Evolution of the amplitude of (1) secondary charging voltage V_{C2} and (2) output load voltage V_R, both as a function of the input voltage V_{C1}.

For an input voltage in the range from 3 kV to 5 kV, no magnetic field H_0 is applied since the induction swing is higher than required for obtaining an efficient transfer of the energy from the primary to the secondary capacitor. This causes the SPT to operate in the late saturation state and, consequently, part of the energy is transferred back to the primary. A magnetic field of the same direction as the main pulse could have been applied to regulate the induction swing in order to optimize the overall energy efficiency of the generator at these operation points (from 3 kV to 5 kV). The range of adjustment can also be extended by increasing the voltage capability of the primary capacitor C1.

C. Nanosecond High-Voltage Generator Based on SOS-180-4 and Finemet FT-3H

For this generator, the electrical circuit and parameters are the same as presented in Fig. 1 and TABLE I. The SPT of transformation ratio 10 is based on the Finemet FT-3H core (see TABLE II). The generator is designed to operate at a fixed input voltage V_{C1} of 10 kV. The bias field H_0 of 1.5 A/m is required for an operation at the optimum saturation of the core. This applied magnetic field is only 2.5 times higher than the coercive force but is strong enough to properly bias the square B-H loop core. In such conditions, the effective induction swing of the core is evaluated as ~2.2 T.

Fig. 9 illustrates the SOS current and the load voltage impulse obtained for a load of 1 kΩ. To prevent breakdown, both the diode and the load are immersed in oil. The amplitude and duration of the forward current are 620 A and 430 ns, respectively. The reverse current has a duration of 86 ns and an amplitude of 2 kA. A diode cut-off time of 22 ns is measured. The transformer compression ratio, defined as the ratio of the SOS forward pumping current duration to twice the reverse pumping time ($t^+/2t^-$), is evaluated as 2.5. The ratio of the forward to reverse current amplitude (I^+/I^-) is more than 3. A load voltage pulse is generated, having an amplitude of 210 kV, a rise time of 16 ns and an FWHM of 32 ns. The charging voltage V_{C2} of the secondary capacitor is measured as 85 kV. The overvoltage coefficient k_{ov} of the SOS, defined as the ratio of the output voltage V_R to the charging voltage of C2, is 2.5.

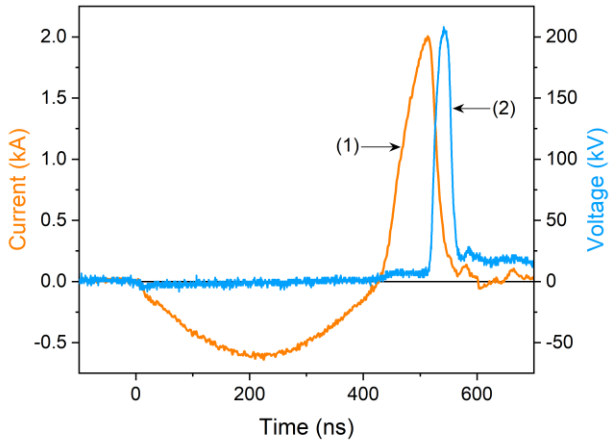

Fig. 9. Waveforms of (1) the current flowing through the SOS diode I_{SOS} and (2) the load voltage V_R for R = 1 kΩ, for the generator based on the Finemet FT-3H core.

The influence of the load upon the operation of the generator was also studied for resistive loads varied between 50 Ω and 1 kΩ. In what follows, the energy switching efficiency of the SOS diode is defined as the ratio of the energy transmitted to the load R to the energy stored in the secondary capacitor C2 ($\eta_{SOS} = E_R/E_{C2}$). The load peak power is calculated from the load voltage V_R measured experimentally.

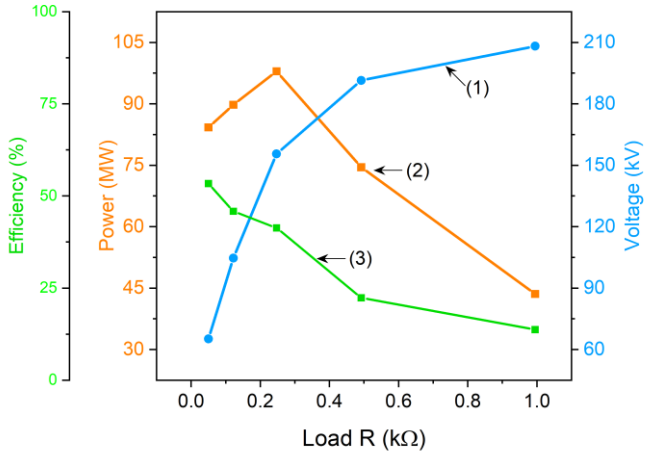

Fig. 10. Load characteristic of the generator based on the Finemet FT-3H core: (1) load voltage V_R, (2) peak power P_R, and (3) diode energy switching efficiency η_{SOS} for different values of resistive load ranging from 50 Ω to 1 kΩ.

The main results are presented in Fig. 10. A peak output power P_R of ~100 MW is obtained with a load of 250 Ω while the maximum voltage of ~210 kV is obtained for a 1 kΩ load. The

change in the load does not influence the transformer efficiency η_{PT} which is superior to 70% for each load (up to 77% at 1 kΩ).

The diode energy switching efficiency reaches its maximum of 54% with the load of 50 Ω and its minimum of only 16% for the load of 1 kΩ (Fig. 10). Considering that the energy efficiency is highest when the source and load impedances match, a higher efficiency should be reached by matching the source impedance, estimated as 32 Ω. On the contrary, the overvoltage coefficient is maximum (k_{ov} = 2.5) for 1 kΩ and minimum (k_{ov} = 0.8) for the 50 Ω load. This result is in agreement with [2], which reports that the switching efficiency of SOS decreases with the increase of the overvoltage coefficient.

IV. Conclusion

The present paper describes the studies related to optimizing the operation of a saturable pulse transformer when used as part of a pulsed-power high-voltage SOS generator. It was found that the saturation flux density is one of the most critical parameters when designing an SPT. The SPT was studied using nanocrystalline magnetic cores of both flat and square hysteresis loops. The comparison of results obtained with these cores reveals the most important features of a hysteresis loop. Thus, it was found that the core presenting the square hysteresis loop, due to the low magnetic field required for the maximum induction swing, is suitable for an operation at a fixed voltage. On the other hand, when using a flat hysteresis loop core, the generator output voltage can be adjusted almost linearly, by tuning the input voltage and by applying the adequate bias magnetic field. It was also demonstrated that a relatively high DC current amplitude is necessary to generate the required magnetic field for higher voltages while using the flat hysteresis loop core. In such a case, proper cooling of the choke must be considered. Two SOS generators based on the aforementioned cores were designed, manufactured and tested. The control of the bias magnetic field enabled these generators to be operated with a high transformer efficiency of more than 70%. Future research will focus on using a solid-state switch in the primary circuit to improve the overall energy efficiency and address the high pulse repetition frequency operation of these generators. Applying the proposed voltage regulation method to more energetic (>10 J) SOS generators will also be considered.

References

[1] S. K. Lyubutin, G. A. Mesyats, S. N. Rukin, B. G. Slovikovskii, and A. M. Turov, "New solid state opening switches for repetitive pulsed power technology," in *11th International Conference on High-Power Particle Beams*, 1996, pp. 135–138.

[2] S. N. Rukin, "Pulsed power technology based on semiconductor opening switches: A review," *Review of Scientific Instruments*, vol. 91, no. 1, p. 011501, Jan. 2020, doi: 10.1063/1.5128297.

[3] S. Yu. Sokovnin and M. E. Balezin, "Surface irradiation installation for eggs based on URT-0,5M accelerator," *Radiation Physics and Chemistry*, vol. 196, no. January, p. 110137, Jul. 2022, doi: 10.1016/j.radphyschem.2022.110137.

[4] S. Y. Sokovnin and M. E. Balezin, "Repetitive nanosecond electron accelerators type URT-1 for radiation technology," *Radiation Physics and Chemistry*, vol. 144, no. April 2016, pp. 265–270, 2018, doi: 10.1016/j.radphyschem.2017.08.023.

[5] T. Sugai, W. Liu, A. Tokuchi, W. Jiang, and Y. Minamitani, "Influence of a Circuit Parameter for Plasma Water Treatment by an Inductive Energy Storage Circuit Using Semiconductor Opening Switch," *IEEE Transactions on Plasma Science*, vol. 41, no. 4, pp. 967–974, Apr. 2013, doi: 10.1109/TPS.2013.2251359.

[6] G. Wang, J. Su, Z. Ding, X. Yuan, and Y. Pan, "A semiconductor opening switch based generator with pulse repetitive frequency of 4 MHz," *Review of Scientific Instruments*, vol. 84, no. 12, p. 125102, Dec. 2013, doi: 10.1063/1.4833683.

[7] G. H. Rim, B. D. Min, E. Pavlov, and J. H. Kim, "Repetitive Nanosecond All-Solid-State Pulse Generator Using Magnetic Switch and SOS Diodes," in *2005 IEEE Pulsed Power Conference*, IEEE, Jun. 2005, pp. 1069–1072. doi: 10.1109/PPC.2005.300504.

[8] A. B. J. M. Driessen, E. J. M. van Heesch, T. Huiskamp, F. J. C. M. Beckers, and A. J. M. Pemen, "Compact Pulse Topology for Adjustable High-Voltage Pulse Generation Using an SOS Diode," *IEEE Transactions on Plasma Science*, vol. 42, no. 10, pp. 3083–3088, Oct. 2014, doi: 10.1109/TPS.2014.2314686.

[9] S. Lyubutin *et al.*, "High efficiency nanosecond generator based on semiconductor opening switch," *IEEE Transactions on Dielectrics and Electrical Insulation*, vol. 18, no. 4, pp. 1221–1227, Aug. 2011, doi: 10.1109/TDEI.2011.5976119.

[10] A. I. Gusev, S. K. Lyubutin, A. V. Ponomarev, S. N. Rukin, and B. G. Slovikovsky, "Semiconductor opening switch generator with a primary thyristor switch triggered in impact-ionization wave mode," *Review of Scientific Instruments*, vol. 89, no. 11, p. 114702, Nov. 2018, doi: 10.1063/1.5052530.

[11] G. A. Mesyats, *Pulsed Power*. Springer US, 2004. doi: 10.1007/b116932.

[12] T. Sakugawa and H. Akiyama, "An all-solid-state pulsed power generator using a high-speed gate-turn-off thyristor and a saturable transformer," *Electrical Engineering in Japan (English translation of Denki Gakkai Ronbunshi)*, vol. 140, no. 4, pp. 17–26, 2002, doi: 10.1002/eej.2006.

[13] Q. Yuan, Z. Deng, W. Ding, Y. Wang, and J. Wu, "New advances in solid-state pulse generator based on magnetic switches," *Review of Scientific Instruments*, vol. 93, no. 5, p. 051501, May 2022, doi: 10.1063/5.0079583.

[14] D. Zhang, Y. Zhou, J. Wang, and P. Yan, "A compact, high repetition-rate, nanosecond pulse generator based on magnetic pulse compression system," *IEEE Transactions on Dielectrics and Electrical Insulation*, vol. 18, no. 4, pp. 1151–1157, Aug. 2011, doi: 10.1109/TDEI.2011.5976109.

[15] H. Akiyama, T. Sakugawa, T. Namihira, K. Takaki, Y. Minamitani, and N. Shimomura, "Industrial Applications of Pulsed Power Technology," *IEEE Transactions on Dielectrics and Electrical Insulation*, vol. 14, no. 5, pp. 1051–1064, Oct. 2007, doi: 10.1109/TDEI.2007.4339465.

[16] Z. Zhang and X. Tan, "Review of High Power Pulse Transformer Design," *Phys Procedia*, vol. 32, pp. 566–574, 2012, doi: 10.1016/j.phpro.2012.03.602.

[17] L. Rong and Q. Rong, "Research on pulse power based on saturable pulse transformer and magnetic switch," *The Journal of Engineering*, vol. 2018, no. 10, pp. 1384–1388, Oct. 2018, doi: 10.1049/joe.2018.5026.

[18] L. Pecastaing, M. Rivaletto, A. S. de Ferron, R. Pecquois, and B. M. Novac, "Development of a 0.6-MV Ultracompact Magnetic Core Pulsed Transformer for High-Power Applications," *IEEE Transactions on Plasma Science*, vol. 46, no. 1, pp. 156–166, Jan. 2018, doi: 10.1109/TPS.2017.2781620.

[19] S. Li *et al.*, "Investigation on Adjustable Magnetic Pulse Compressor in Power Supply System," *IEEE Trans Power Electron*, vol. 34, no. 2, pp. 1540–1547, Feb. 2019, doi: 10.1109/TPEL.2018.2830106.

[20] J. Choi, "Introduction of the Magnetic Pulse Compressor (MPC) - Fundamental Review and Practical Application," *Journal of Electrical Engineering and Technology*, vol. 5, no. 3, pp. 484–492, Sep. 2010, doi: 10.5370/JEET.2010.5.3.484.

[21] J. Holma and M. J. Barnes, "Prototype Inductive Adders With Extremely Flat-Top Output Pulses for the Compact Linear Collider at CERN," *IEEE Transactions on Plasma Science*, vol. 46, no. 10, pp. 3348–3358, Oct. 2018, doi: 10.1109/TPS.2018.2836310.

[22] M. J. Barnes *et al.*, "Future circular collider injection and extraction kicker topologies and solid state generators," *Physical Review Accelerators and Beams*, vol. 22, no. 7, p. 071001, Jul. 2019, doi: 10.1103/PhysRevAccelBeams.22.071001.

[23] S. R. Korzhenevskiy, A. A. Komarskiy, A. S. Chepusov, V. A. Bessonova, and V. N. Titov, "Output voltage adjustment of a pulsed high-voltage nanosecond generator with inductive energy storage and a solid-state switching system," *Instruments and Experimental Techniques*, vol. 60, no. 1, pp. 46–49, Jan. 2017, doi: 10.1134/S0020441217010213.

[24] R. Burdt, R. D. Curry, K. F. McDonald, P. Melcher, R. Ness, and C. Huang, "Evaluation of nanocrystalline materials, amorphous metal alloys,

and ferrites for magnetic pulse compression applications," *J Appl Phys*, vol. 99, no. 8, p. 08D911, Apr. 2006, doi: 10.1063/1.2173214.
[25] T. Filchev, F. Carastro, P. Wheeler, and J. Clare, "High voltage high frequency power transformer for pulsed power application," in *Proceedings of 14th International Power Electronics and Motion Control Conference EPE-PEMC 2010*, IEEE, Sep. 2010, pp. 165–170. doi: 10.1109/EPEPEMC.2010.5606517.
[26] M. R. Degnon *et al.*, "Off-the-Shelf Diodes as High-Voltage Opening Switches," *IEEE Transactions on Plasma Science*, vol. 50, no. 10, pp. 3384–3392, Oct. 2022, doi: 10.1109/TPS.2022.3177702.
[27] E. A. Alichkin, S. K. Lyubutin, A. V Ponomarev, S. N. Rukin, and B. G. Slovikovskii, "Formation of Short Pulses with a Subnanosecond Rise Time and a Peak Power of Up to 1 GW by a Semiconductor Avalanche Sharpener," vol. 45, no. 4, pp. 535–539, 2002.
[28] "Nanocrystalline Soft Magnetic Material FINEMET® | Hitachi Metals, Ltd." https://www.hitachi.com/ (accessed Dec. 07, 2022).
[29] S. Nakajima, S. Arakawa, Y. Yamashita, and M. Shiho, "Fe-based nanocrystalline FINEMET cores for induction accelerators," *Nucl Instrum Methods Phys Res A*, vol. 331, no. 1–3, pp. 318–322, Jul. 1993, doi: 10.1016/0168-9002(93)90066-Q.

Mawuena R. Degnon (Graduate Student member, IEEE) received the M.Eng. degree in electrical engineering from the Université de Lomé, Lomé, Togo, in 2018, and the M.Sc. degree in electrical engineering and industrial computing from the Université de Pau et des Pays de l'Adour (UPPA), Pau, France, in 2020, where he is currently pursuing the Ph.D. degree in electrical engineering with the Laboratoire des Sciences de l'Ingénieur Appliquées à la Mécanique et au Génie Électrique (SIAME Laboratory) and in collaboration with ITOPP ALCEN.

His research interests include high-voltage pulsed power systems, high-power solid-state switches, and nanosecond high-voltage generators. He has received the Outstanding Young Researcher Award at the Euro-Asian Pulsed Power Conference (EAPPC) in 2021.

Anton I. Gusev (Member, IEEE) was born in Miass, Russia, in 1988. He received the M.S. degree in electrophysics from Ural Federal University (UrFU), Yekaterinburg, Russia, in 2012, and the Ph.D. degree in engineering sciences from the Institute of Electrophysics (IEP), Ural Branch of the Russian Academy of Sciences, Yekaterinburg, in 2019. From 2008 to 2019, he was an Intern, a Ph.D. Student, and a Junior Researcher with the Pulsed Power Laboratory, IEP. From 2014 to 2019, he was with UrFU as a Senior Teacher. In 2019, he became a Post-Doctoral Researcher with the Université de Pau et des Pays de l'Adour (UPPA), Pau, France, where he has been an Assistant Professor with the Laboratoire des Sciences de l'Ingénieur Appliquées à la Mécanique et au Génie Électrique (SIAME) since 2020.

His research interests include semiconductor physics, high-power semiconductor switches, and high-voltage solid-state generators, which provide nano and subnanosecond pulses.

Dr. Gusev is a member of the International Society on Pulsed Power Applications (ISP) and the Association for the Advancement of Pulsed Power (A2P2). He has received the Outstanding Young Researcher Award at major international pulsed power conferences (the Energy Fluxes and Radiation Effects (EFRE) in 2016, the Euro-Asian Pulsed Power Conference (EAPPC) in 2018, and the Gas Discharge Plasmas and Their Applications (GDP) in 2021), including two IEEE-supported conferences: the IEEE Pulsed Power Conference (PPC) in 2017 and the IEEE International Power Modulator and High Voltage Conference (IPMHVC) in 2018.

Antoine Silvestre de Ferron was born in Tarbes, France, in 1977. He received the master's degree in electrical and electronic engineering from the University of Toulouse, Toulouse, France, in 2002, and the Ph.D. degree in electrical engineering from the Université de Pau et des Pays de l'Adour (UPPA), Pau, France, in 2006. From 2006 to 2008, he was a Researcher with the Commissariat à l'Energie Atomique (CEA), Le Barp, France, a French government-fund technological research organization. He is currently an Engineer with the Head of the High-Voltage Processes Team, Laboratoire des Sciences de l'Ingénieur Appliquées à la Mécanique et au Génie Électrique (SIAME Laboratory), UPPA. His research interest includes high pulsed power generation with military and civil applications. He is specialized in Marx generator and pulse forming lines in high-voltage generation, high-voltage transient probes associated, and high-current discharges in liquids.

Laurent Pecastaing (Senior Member, IEEE) received the Ph.D. and Research Directorship Habilitation degrees in electrical engineering from the Université de Pau et des Pays de l'Adour (UPPA), Pau, France, in 2001 and 2010, respectively.

He is currently a Full Professor of pulsed power with UPPA. He is also the Director of the Laboratoire des Sciences de l'Ingénieur Appliquées à la Mécanique et au Génie Électrique (SIAME Laboratory) and the common laboratory between UPPA and the Commissariat à l'Energie Atomique (CEA), Le Barp, France. His current research interests include high-power microwave sources, compact pulsed power systems, and ultrafast transient probes.

Dr. Pecastaing was the Chairperson of the Euro-Asian Pulsed Power Conference/High-Power Particle Beams/Megagauss Magnetic Field Generation and Related Topics (EAPPC/BEAMS/MEGAGAUSS) Conference, France, in 2021. He is also a member of the International Steering Committees for both the BEAMS Conferences and the Euro-Asian Pulsed Power Conferences.

Aleksandr Baranov received the M.Eng. degree in industrial electrical energy and engineering from Togliatti State University, Togliatti, Russia, in 2015. He is currently a Research and Development Engineer with ITOPP ALCEN, Thégra, France.

His research fields of interests are high-voltage nanoseconds' generators, electron emission, and pulsed power systems.

Christophe Mielot was born in 1976 in the north of France. He received the M.Eng. degree in energy and environment in 1999, graduated from INSTN school from the Commissariat à l'Energie Atomique (CEA) in 2000 and received the Ph.D. degree in physics of scientific instruments from Orsay University in 2004.

He spent 15 years as accelerator expert (linac and betatron) for x-ray cargo scanning company. He joined ITOPP ALCEN in 2021 as project manager for the development of a pulsed electron generator based on resonating transformer technology.

Sébastien Boisne was born in Thionville, France, in 1979. He received the master's degree in global management of organizations, strategy, and finance from the University of Paris Dauphine PSL, Paris, France, in 2016.

In 2002, he joined Thomson CSF Linac, Orsay, France, a Leader in linear electron accelerators, where he was in charge of the development of electron beam range of products, intended to be employed in high-demand industrial uses. He is currently with the Head of BETA BEAMS, ITOPP ALCEN Group, Donzenac, France, specializing in the design and supply of electron beam accelerators, installed on end-users' production sites, and mainly used in surface and core sterilization of pharmaceutical products.

Michael J. Barnes received the B.Sc. degree in electrical engineering in 1981. Subsequently he carried out an industrially based Ph.D. in power electronics, with research and development undertaken at the General Electric Company of England (GEC) and academic work at the University of Aston in Birmingham, U.K., and received the Ph.D. degree in 1985. He moved to TRIUMF, Canada, in 1989: the main focus of his work at TRIUMF was in the area of pulsed power kicker systems for use in particle accelerators. Michael joined CERN, Switzerland, in 2006 where he is responsible for several kicker systems, including the high precision injection kicker systems for the Large Hadron Collider (LHC). In addition, he is actively involved in several international collaborations.

Viliam Senaj received his M.Sc. degree in physical electronics in 1986 at Comenius University in Bratislava, Slovakia. He carried his Ph.D. at Institute of Measurement Science of Slovak Academy of Sciences in Bratislava, Slovakia in the domain of generation and measurement of magnetic field gradients for magnetic resonance imaging, where he received his Ph.D. degree in 1993. He worked on several international projects - at Centre National de la Recherche Scientifique in Orsay, France on generation and precise measurement of magnetic field gradients for MR imaging of lungs with hyperpolarized He3. At Commissariat à l'Energie Atomique (CEA) Saclay, France he worked on specification of the magnetic field gradient system for the world largest MRI scanner for functional magnetic resonance imaging. In 2006 he shortly worked at Honeywell Aerospace in switched mode power supply design office at Bratislava, Slovakia.

In 2007 he joined CERN, Switzerland where he is responsible for beam dump generators of the Super Proton Synchrotron and the Large Hadron Collider accelerators.

Thomas Kramer received the Diploma degree in electrical and biomedical engineering in 2004 from the Graz University of Technology, Austria. Subsequently he carried out a Ph.D. at the same university and in collaboration with the European Organization for Nuclear Research (CERN, Switzerland). He received the Ph.D. degree in 2011 with distinction for his work on the Large Hadron Collider beam extraction system.

From 2009 to 2012 he was with EBG MedAustron designing and implementing the beam transfer elements for this medical ion accelerator. Thomas joined CERN's beam transfer group in 2012 as electrical engineer for operation, maintenance and development of fast pulsed magnet systems. Since 2017 he is leading the pulsed power engineering section in the same group.

Bucur M. Novac (M'06 – SM'08) received the M.Sc. and Ph.D. degrees in 1977 and 1989, respectively, both from the University of Bucharest. He joined the Loughborough University, UK in 1998 and is currently Professor of Pulsed Power. His research interests include compact and repetitive high-power systems,

explosively and electromagnetically driven magnetic flux compression generators and their applications, exploding wire technology, electromagnetic launchers, high-power underwater plasma discharges, ultrafast magneto and electro-optic sensors and 2-D modeling of pulsed-power systems. He has co-authored two books on explosive pulsed power and has published more than 200 refereed papers and conference contributions.

He is a member of the International Steering Committees for both the MEGAGAUSS Conferences and for the Euro-Asian Pulsed Power Conferences. Prof. Novac is a voting member of the Pulsed Power Science & Technology Committee in the IEEE Nuclear and Plasma Science Society and a member of the organizing committee for the IEEE International Power Modulator and High Voltage Conference, as well as chairperson of the UK Pulsed Power Symposia.

Prof. Novac is a Fellow of the Royal Academy of Engineering, a Chartered Engineer and a Fellow of The Institution of Engineering and Technology, UK.